JOURNAL OF MATERIALS SCIENCE 22 (1987) 4133–4138

Extruded ceramic fibres of modified lead titanate including sol–gel precursors

L. DEL OLMO, L. PARDO, J. I. PINA, J. MENDIOLA
Instituto de Ciencia de Materiales. C.S.I.C. Serrano, 144, 28006 Madrid, Spain

An original procedure to obtain extruded ceramic fibres of calcium modified lead titanate has been developed. Slurry preparation was made by homogeneous mixture of crystalline ceramic powder with a gel of analogous composition acting as plasticizer. In addition, the gel phase provides a binder effect to the green fibres after extrusion and during the first stage of the firing process. On the other hand, the high reactivity of the gel accelerates the sintering mechanisms. Fibres of ~1 mm final diameter and 97% of the theoretical density were obtained for moderate sintering conditions (1000° C, 3 to 7 h). The microstructure of the fibres was studied in comparison with those of ceramics prepared from each of the two components separately. Since electromechanical properties of these types of ceramics strongly depend on the microstructure, the procedure here developed is considered very appropriate for their processing.

1. Introduction

Ceramics of the system TiO_2–PbO–CaO present interesting properties as piezoelectric transducers in the ultrasonic range due to their high electromechanical anisotropy [1]. Reactive processes by sol–gel techniques have been developed effectively during the last few years [2, 3] for the preparation of inorganic precursors, and have enhanced the quality of the ceramics. As is the case in the present work, incorporation of amorphous phases (gels) may solve certain difficulties during processing, acting as an alternative to conventionally used materials.

In this work a procedure has been developed to obtain ceramic fibres of calcium-modified lead titanate. The extrusion moulding is the most appropriate method for this purpose. Considering the high densification and purity requirements of this type of ceramics, a method is proposed here to prepare the slurry for extrusion moulding. A gel with analogous composition to that of the ceramic powder is used as plasticizer. This method has the advantage of eliminating the volatilization step of the conventional organic plasticizers during the firing of the fibres. The undesirable development of pores and cracks is thus avoided.

Due to the high effectiveness of its plasticizer action, the gel is a relatively low percentage of the composition of the slurry. This fact allows firing to proceed without a previous synthesis of the gel. In this way a reactivation of the system is achieved which accelerates the sintering reactions.

The processing of ceramic fibres is useful in the preparation of composite materials, since PZT fibres composites [4, 5] have been tested as ultrasonic transducers and have shown certain advantages in comparison with single ceramics transducers.

2. Experimental procedures

The fibre processing was studied as follows.

2.1. Slurry components

The slurry for extrusion moulding was prepared with the two following components:

1. Component A was a ceramic powder with the composition

$$Pb_{0.76}Ca_{0.24}[(Co_{0.5}, W_{0.5})_{0.05}Ti_{0.95}]O_3 + 1\ \%\ MnO \quad (1)$$

which has a tetragonal perovskite structure at room temperature according its X-ray diffraction (XRD) pattern (Fig. 1a). This compound was the result of a reactive synthesis [6] at 900° C for 3 h.

2. Component B was a gel (Fig. 1b) made from a homogeneous mixture of amorphous hydrated oxides ($MO_m(OH)_n$, M = metal), which was prepared by sol–gel process. It is characterized by a composition analogous to that of component A with an excess of 2% of PbO by weight. Component B was prepared from high purity inorganic raw materials (nitrates, carbonates and chlorides) by the sol–gel process, summarized in Fig. 2. It was dried at 100° C for 16 h and was incorporated to the slurry with component A after deagglomeration.

The reactivity and other physical–chemical characteristics of component B are deduced from its thermogravimetry (TG), differential thermogravimetry (DTG) and differential thermal analysis (DTA) curves (Figs 3 and 4). The beginning and development of gel crystallization were monitored by XRD after thermal treatments at different temperatures for 1 h (Fig. 5). The first crystalline phases appear at 450° C. This value is close to that observed by other authors for unmodified lead titanate prepared by sol–gel from metal alkoxides [7].

2.2. Extrusion moulding

Using component B (gel) as plasticizer, a mixture with

0022–2461/87 $03.00 + .12

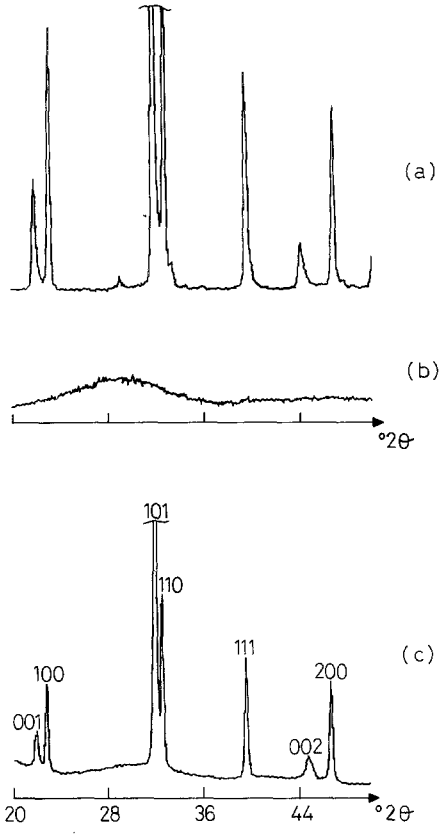

Figure 1 XRD pattern of (a) crystalline ceramic powder of modified lead titanate (component A), (b) gel of analogous composition (component B) and (c) sintered fibre.

component A (ceramic powder) and deionized water was made by ball-milling in a tungsten mill. Different ratios by weight between the two solid components of the slurry were tested (Table I). The best composition for our purpose was A : B = 9 : 1.

The optimum solid : water ratio of the slurry was also studied and was found to be 17% water content. In addition to this water, a content of adsorbed water remains in the gel after drying at 100° C for 16 h, according to its TG curve (Fig. 3).

With the above-mentioned composition, a slurry

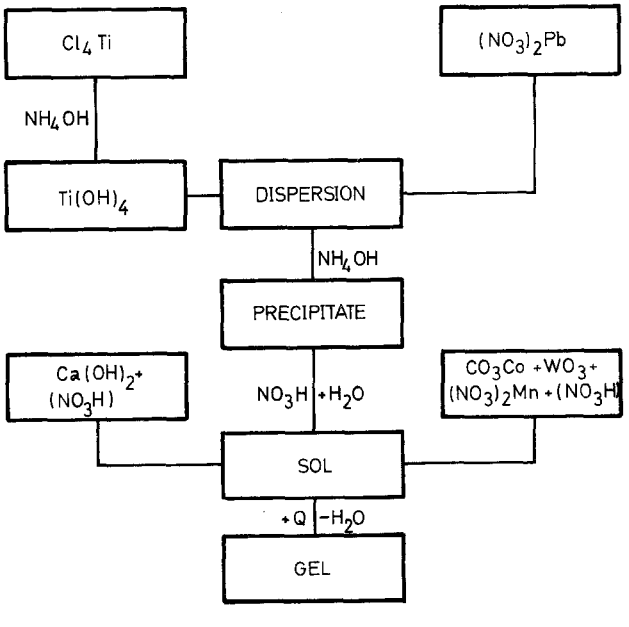

Figure 2 Block diagram of the sol–gel process.

TABLE I Percentage of deionized water in the slurry to be extruded and percentage volume contraction of the fibres after extrusion, during drying, as a function of the weight ratio between components A and B of the slurry

A : B	% H_2O	vol % contraction
50 : 50	35	27
75 : 25	28	19
90 : 10	17	14

was obtained that, once extruded, gave place to green fibres with diameters in the millimeter range. These fibres had good mechanical stability and presented homogeneous shrinkage that did not damage them during drying at 60 to 70° C under infrared radiation.

2.3. Firing

After drying, fibres were fired in an electric furnace, in air atmosphere and on an inert substrate. The firing program was as follows:

1. a heating ramp from room temperature to the sintering temperature at a rate of 6° C min^{-1};
2. a plateau at this temperature during a variable time; and
3. cooling ramp to room temperature with the furnace turned off.

Table II shows the densification results for the different sintering times and temperatures that were tested.

The firing program does not require any special care in the first part of the process. This suggests that the gel acts as a binder while remaining in an amorphous state below 450° C (Fig. 5). Synthesis reactions and crystallization of the gel develop from this temperature up to 700 to 800° C, when the sintering mechanisms begin to act.

The best results of densification (97% of theoretical density) were obtained for sintering conditions of 1000° C, 3 to 7 h. The diameter shrinkage during firing was 22%.

2.4. Characterization and properties

We will refer only to fibres obtained for the conditions that were determined as optimum in the preceding sections, i.e. the ratio between slurry solid components A : B = 9 : 1 and sintering conditions of 1000° C, 3 to 7 h.

Sintered fibres have an XRD pattern (Fig. 1c) that

TABLE II Density and corresponding densification of the sintered fibres as a function of different sintering temperatures and times

T_{sint} (°C)	t_{sint} (h)	ϱ (g cm^{-1})	Densification (%)
950	7	6.49	90
1000	3	6.94	97
1000	7	6.97	97
1000	10	6.63	92
1050	3	6.54	91
1050	10	6.62	92
1100	10	6.69	93
1150	7	6.24	87

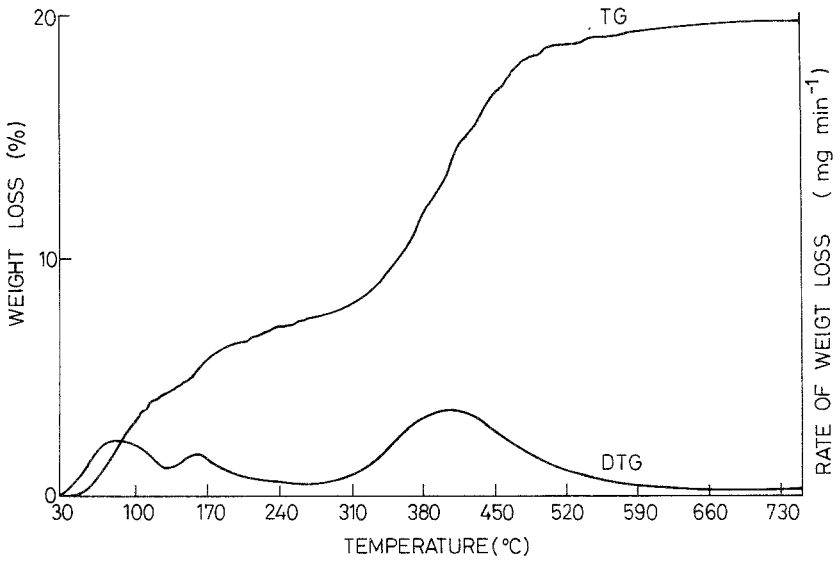

Figure 3 TG and DTG analysis curves for the dry gel. Scan rate = 8 deg min^{-1}.

corresponds to a perovskite structure with tetragonal distortion at room temperature of c:a = 1.039, which adjusts to the designed composition. The XRD pattern does not show the presence of non-reacted products or other crystalline phases.

The micrograph of the fibres obtained by scanning electron microscopy (SEM) on a fracture surface (Fig. 6c) reveals the intergranular nature of the fracture. Micrographs of ceramics prepared separately from components A and B by isostatic press moulding are also presented for the sake of comparison (Figs 6a and b).

Two aspects of the fracture surface of the fibres was analysed by Auger electron spectroscopy (AES).

2.4.1. Qualitative analysis of component elements

The AES spectra obtained for the fracture surface (Fig. 7) shows only the presence of the main elements ot the system. The small peak of carbon, in addition to a contamination usual in this type of analysis, may have its origin in this case in an incomplete combustion of the isopropyl alcohol used in deagglomeration of precursors.

2.4.2. Depth compositional profile analysis

Fig. 8 shows the change of the Auger peak relative intensities for each element, taking as reference the main titanium peak, as a function of the ionic bombardment time of the surface. Auger peak intensities in the spectra are related with element concentrations in the studied surface. The area analysed for each point corresponds to a 100 μm diameter zone. Since fracture was intergranular (Fig. 6c), an average depth compositional profile for hundreds of grains was obtained going from grain boundaries to the bulk of the grains as ionic bombardment time increases and the surface is eroded.

Segments of the fibres of 1.4 mm final diameter (Fig. 9) and ~4 mm length were electroded and poled under fields of 60 kV cm^{-1}. Results of their ferroelectric (Fig. 10) and piezoelectric characterization are shown in Table III. The parameters that correspond to thickness and planar vibration modes of thin discs were obtained for discs of pressed and fired dry slurry.

3. Results and discussion

The experiments show that the incorporation of an inorganic amorphous phase (gel) in homogeneous

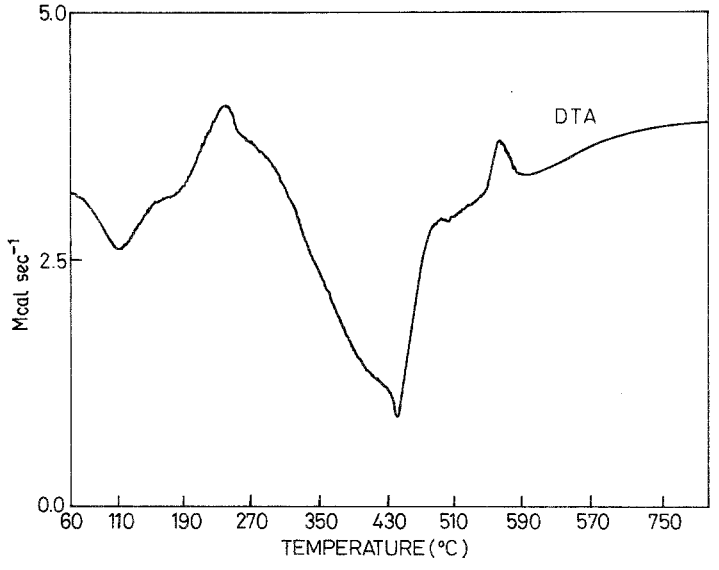

Figure 4 DTA curve for the dry gel. Scan rate = 8 deg min^{-1}.

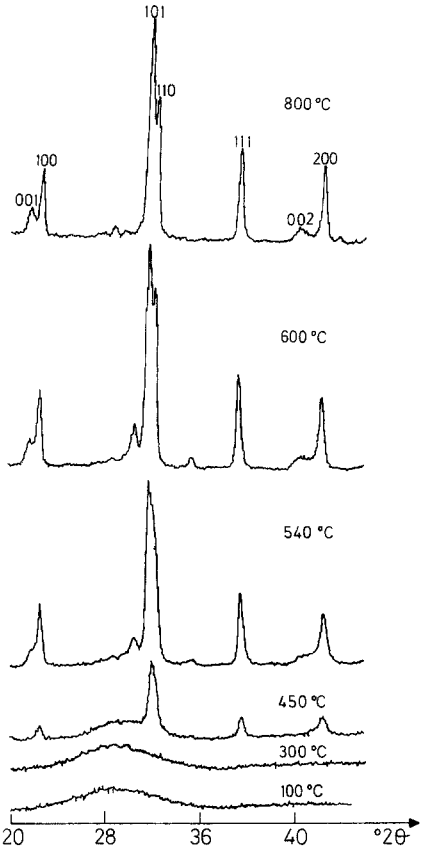

Figure 5 XRD pattern of the dry gel after thermal treatments for 1 h.

TABLE III Ferroelectric and piezoelectric parameters for the sintered fibres obtained from a slurry with solid composition corresponding to the ratio by weight A : B = 9 : 1

$T_{\varepsilon'_{max}}$ (°C)	276
ε' (1 kHz, 22° C)	160–182
D(1 kHz, 22° C)	0.012–0.011
P_R (μC cm^{-2})	32.5–34.5
d_{33}(pC N^{-1})	54–60
g_{33}($\times 10^{-3}$ m V N^{-1})	34–38
K_p	$\simeq 0$
K_t	45–47
N_t(Hz m)	1850–2200
Q_m	120–20

mixture with the crystalline ceramic powder leads to a slurry that fulfils the compromises encountered during the fibre processing.

10% gel incorporated in the solid content of the slurry provides the needed plasticity for extrusion by adjustment of the humidity content to 17% water. The gel also has a binder action in the green fibres. Thus it avoids the 14% volume contraction damage during drying.

This binder action of the gel extends to the first part of the firing process, while the gel remains in an amorphous state below ~450° C. It is in this temperature interval when the gel, dried at 100° C for 16 h, presents three different dehydration processes according to its DTA (Fig. 4). These take place at 110, 180 and 430° C, where three endothermic peaks appear in the curve. The first two dehydration stages correspond to a 4.3% and 2.9% weight loss, values obtained from the TG analysis curve (Fig. 3). The third, which is more intense, coincides with the beginning of formation of the first crystalline phases in the gel after thermal treatments of 1 h (Fig. 5). It also corresponds to the beginning of a 12.4% weight loss through an interval that extends to 700° C. In this interval the gel shows a crystallization temperature of 560° C by an exotherm peak in the DTA curve, that is close to the one found by other authors [8] for unmodified lead titanate.

The XRD patterns for the dry gel after thermal treatments of 1 h (Fig. 5) show that, in addition to the

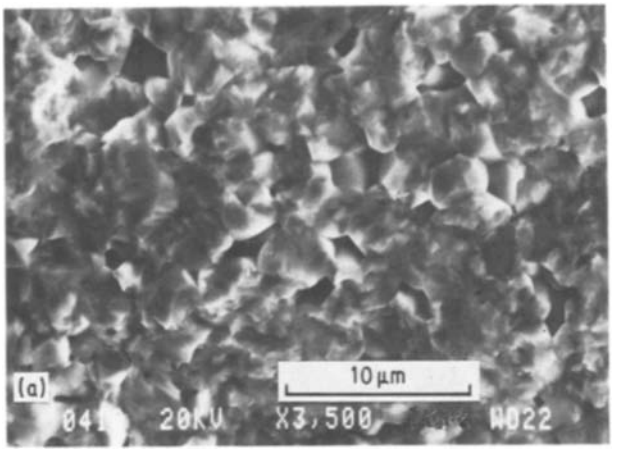

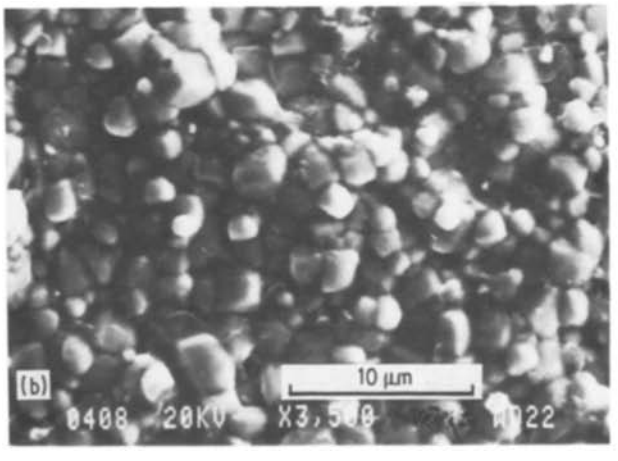

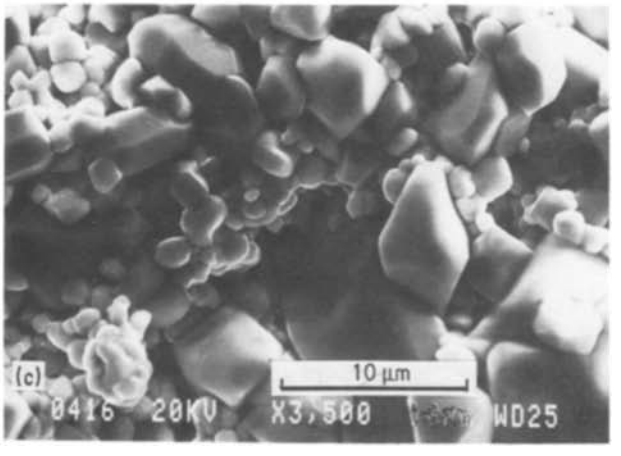

Figure 6 SEM micrographs on a fracture surface of ceramics obtained from (a) component A, (b) component B and (c) of a sintered fibre.

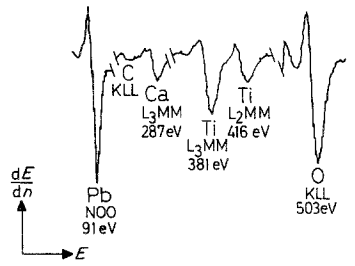

Figure 7 Auger electron spectra on the fracture surface of a sintered fibre [9].

main diffraction peaks corresponding to the modified lead titanate, the gel presents diffraction peaks with interplanar distances $d = 0.291$ and 0.253 nm. These additional peaks are associated with transient phases that present the maximum development at 600° C and disappear at 800° C. At this temperature the gel is totally crystallized and has a tetragonal distortion of $c/a = 1.042$. This value is slightly higher than that corresponding to a stoichiometry PbO : CaO = 76 : 24 and could be related to the 2% excess lead of the gel.

Although the above-mentioned synthesis and crystallization processes occur in the gel during firing of the fibres, the former are not altered due to the relatively small percentage of gel that is incorporated. On the contrary, the reactive phase (gel) provides an acceleration of the sintering mechanisms that give place to fibres of 97% densification and 1.4 mm final diameter for moderate sintering conditions (1000° C, 3 to 7 h).

The gel distributes around the particles of the ceramic powder during mixing and extruding and gives place to a microstructure that remains in the final ceramic.

The micrograph showing Fig. 6c shows the presence in the fibres of two types of grains, which have different grain sizes. The grains of $\sim 10\,\mu$m size correspond to component A, whereas those of 1 to 2 μm have origin in component B and are the result of its crystallization during firing of the fibres.

For the ceramic processed exclusively from component A, fracture is transgranular (Fig. 6a), whereas it is intergranular for the ceramic processed from component B. Fracture also occurs intergranularly in the sintered fibre (Fig. 6c) and mainly through grains generated in component B. These grains have a similar

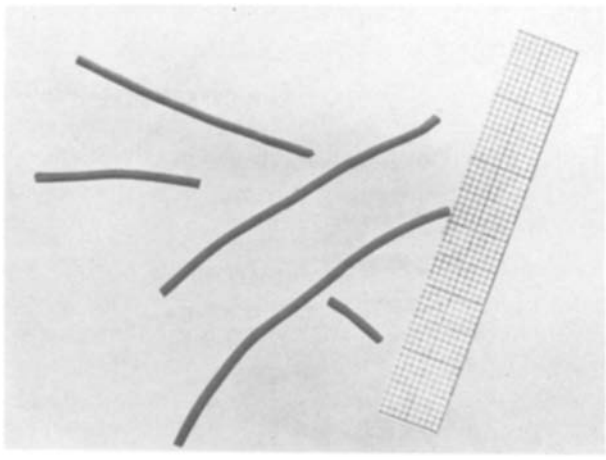

Figure 9 Sintered fibres obtained by extrusion.

grain size in the fibres and in the ceramic prepared only from component B. On the contrary, the grains of $\sim 3\,\mu$m size that appear in the ceramic prepared from component A have higher development in the fibres and a grain size of $\sim 10\,\mu$m is obtained.

The grain growth in the fibres is related to the reactivation of the sintering mechanisms caused by the presence of the gel. This phase, due to its reactive nature and slight excess of PbO, constitutes the main component of the interphases or grain boundaries created during firing. Such interphases have a composition rich in PbO, determined by AES techniques (Fig. 8). Solid solutions, which have a stoichiometry that corresponds to component A [7], are stabilized in the bulk of the grains.

This interphase, relatively wide and rich in PbO, favours sintering and constitutes the preferential fracture surface. On the other hand, it provides sinks for the excess PbO of the fibres that is provided by the gel. In this way, the PbO does not incorporate the solid solution that constitutes the bulk of the grains, as the tetragonal distortion of the fibres ($c/a = 1.039$) indicates. The absence of two different perovskites with their origin in each of the two components of the slurry is also supported by the behaviour of the relative permitivity of the fibres, K', as a function of temperature (Fig. 10) in the vicinity of the ferro-paraelectric transition. This curve presents only a maximum of K', i.e. the existence of only one transition temperature. The soft widening of the peak is usual in ceramics and the curve does not show other anomalies.

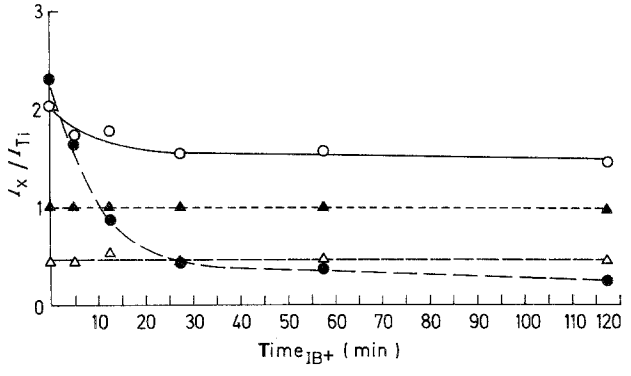

Figure 8 Depth profile analysis obtained by AES on the fracture surface of a sintered fibre [9]. ○, O; ▲, Ti; △, Ca; ● Pb.

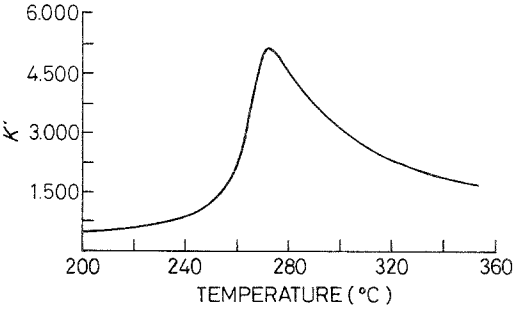

Figure 10 Relative permittivity of the fibres in the vicinity of the ferro-paraelectric transition.

Therefore, the microstructure of the ceramic fibres has two main characteristics.

1. Two types of grains of different grain size but the same composition and crystalline structure, each coming from one of the two components of the slurry.
2. Interphases between grains that are relatively wide and rich in PbO.

Experiments carried out for ceramics processed by different methods [10] show that these interphases between grains rich in PbO favour the elimination of the electromechanical coupling coefficient for planar vibrations in thin discs. This is very interesting for ultrasonic transducers that are used in ecographic applications. According to the microstructural study presented here for the fibres, the developed procedure seems to be very promising for the controlled generation of such interphases during processing of these ceramics.

4. Conclusions

1. A procedure has been developed to obtain extruded ceramic fibres with ~ 1 mm diameter of a pure oxide material, calcium-modified lead titanate, without the incorporation of conventional organic plasticizers.

2. The use as plasticizer of a gel with analogous composition to the final ceramic provides a binder effect to the extruded green fibre after extrusion and during the first stage of firing. The gel also favours a reactive synthesis that gives place to fibres with 97% of the theoretical density for moderate sintering conditions (1000° C, 3 to 7 h).

3. The homogeneous distribution of the gel between the crystalline grains in the slurry gives place to a microstructure of the sintered fibres that differs for those obtained for each component. This microstructure relates to the electromechanical properties of the ceramics, which makes the procedure potentially very useful for their processing.

Acknowledgements

The authors wish to thank Dr P. Adeba from the Electron Microscopy Department of the National Center of Metallurgical Research (CENIM) for providing the SEM micrographs.

References

1. Y. YAMASHITA, K. YOKOYAMA, H. HONDA and T. TAKAHASHI, *Jpn J. Appl. Phys.* **20** (1981) 183.
2. J. L. WOODHEAD, *Sci. Ceram.* **13** (1985) 3.
3. D. W. JOHNSON, *J. Amer. Ceram. Soc. Bull.* **60** (1981) 221.
4. L. J. BOWEN and T. R. GURURAJA, *J. Appl. Phys.* **51** (1980) 5661.
5. H. TAKEUCHI and C. NAKAYA, *Ferroelectrics* **68** (1986) 53.
6. L. DEL OLMO, C. FANDINO, J. I. PINA, C. ALEMANY, J. MENDIOLA, L. PARDO, B. JIMENEZ and E. MAURER, Patente Espanola de Invenciòn #555469, Mayo, 1986.
7. J. B. BLUM and S. R. GURKOWICH, *J. Mater. Sci.* **20** (1985) 4479.
8. M. TAKASHIGE, T. NAKAMURA, H. OZAWA, R. UNO, N. TSUYA and K. I. IRAI, *Jpn J. Appl. Phys.* **19** (1980) L225.
9. L. PARDO, J. I. PINA and J. L. SACEDON, *J. Mat. Sci.* **23** (1988) in press.
10. J. MENDIOLA, C. ALEMANY, L. PARDO, B. JIMENEZ, L. DEL OLMO and E. MAURER, *J. Mater. Sci.* **22** (1987) in press.

Received 14 January
and accepted 1 April 1987